JOURNAL OF GEOPHYSICAL RESEARCH, VOL. 112, B04102, doi:10.1029/2006JB004550, 2007

History of the Cretaceous Osbourn spreading center

Nathan J. Downey,[1] Joann M. Stock,[1] Robert W. Clayton,[1] and Steven C. Cande[2]

Received 7 June 2006; revised 5 October 2006; accepted 1 November 2006; published 6 April 2007.

[1] The Osbourn Trough is a fossil spreading center that rifted apart the Manihiki and Hikurangi Plateaus during Cretaceous time. Previous models of the Osbourn spreading center are based on data collected near the trough axis, and therefore only constrain the history of the Osbourn spreading center during the last few Ma of spreading. Our data set includes multibeam data collected northward to the Manihiki Plateau, allowing us to examine seafloor morphology created during the entire active period of the Osbourn spreading center, as well as several additional multibeam data sets that provide the opportunity to examine the relationship between the Osbourn paleospreading center and the Cretaceous Pacific-Phoenix ridge. The axial gravity of the trough is similar to the gravity found at other extinct slow-intermediate spreading rate ridges. Magnetic field measurements indicate that spreading at the trough ceased during Chron C34. Abyssal-hill trends indicate that spreading during the early history of the Osbourn spreading center occurred at 15°–20°. The east-west component of this spreading explains the modern east-west offset of the Manihiki and Hikurangi Plateaus. Spreading rotated to 2°–5° prior to extinction. Abyssal-hill RMS amplitudes show that a decrease in spreading rate, from >7 cm/yr to 2–6 cm/yr full-spreading rate, occurred ~2–6 Ma prior to ridge extinction. Our data analysis is unable to determine the exact spreading rate of the Osbourn spreading center prior to the slowing event. The temporal constraints provided by our data show that the Osbourn spreading center ceased spreading prior to 87 Ma or 93 Ma, depending on whether the Manihiki and Hikurangi Plateaus rifted at 115 Ma or 121 Ma. Our model resolves the conflict between regional models of Osbourn spreading with models based on trough characteristics by showing that spreading at the Osbourn spreading center was decoupled from Pacific-Phoenix spreading.

Citation: Downey, N. J., J. M. Stock, R. W. Clayton, and S. C. Cande (2007), History of the Cretaceous Osbourn spreading center, *J. Geophys. Res.*, *112*, B04102, doi:10.1029/2006JB004550.

1. Introduction

[2] The Osbourn Trough is a fossil Cretaceous spreading axis located in the Southwest Pacific Basin (Figure 1). It lies between the Manihiki and Hikurangi Plateaus, and intersects the Tonga-Kermadec Trench and Louisville Ridge at its western boundary. The Osbourn Trough was identified relatively recently [*Lonsdale*, 1997] due to a weak bathymetric expression, an absence of magnetic field reversal anomalies, and a lack of ship track data. The drilling vessel *Glomar Challenger* surveyed the Osbourn Trough at 26°S, 169°W during Deep Sea Drilling Program (DSDP) leg 91 [*Menard et al.*, 1987]. At the time of this survey the length of the Osbourn Trough was unknown, making its interpretation difficult. Global gravity data sets showed that the trough is characterized by a negative axial gravity anomaly, revealing the full extent of the Osbourn Trough for the first time [*Lonsdale*, 1997; *Sandwell and Smith*, 1997].

[3] *Lonsdale* [1997] hypothesized that the Osbourn Trough is an extinct spreading center, but that result was controversial due to limited data coverage [e.g., *Small and Abbott*, 1998]. Subsequent ship track studies [*Billen and Stock*, 2000], however, showed that the trough has morphology typical of extinct spreading ridges. The Osbourn paleospreading center formed when a large oceanic plateau rifted into several pieces, resulting in the creation of the Manihiki and Hikurangi plateaus [*Lonsdale*, 1997], a hypothesis that is supported by studies of the two plateaus [*Hoernle et al.*, 2004; *Mortimer and Parkinson*, 1996; *Taylor*, 2006]. *Mortimer et al.* [2006] present isotopic data which constrain this rifting event to prior to 115 Ma. Spreading at the Osbourn ridge presumably ceased when the Hikurangi plateau collided with the Chatham Rise paleosubduction zone [*Lonsdale*, 1997].

[4] The spreading rate and extinction age of the Osbourn paleospreading center remain controversial. Data collected at the trough axis imply a slow spreading rate and a late extinction age for the Cretaceous Osbourn spreading center. Conversely, attempts to determine the role the Osbourn spreading center plays in the tectonic history of the Southwest Pacific Basin [*Eagles et al.*, 2004; *Larter et al.*, 2002] require either a fast spreading rate for the Osbourn ridge,

[1] Seismological Laboratory, California Institute of Technology, Pasadena, California, USA.
[2] Scripps Institution of Oceanography, La Jolla, California, USA.

0148-0227/07/2006JB004550$09.00

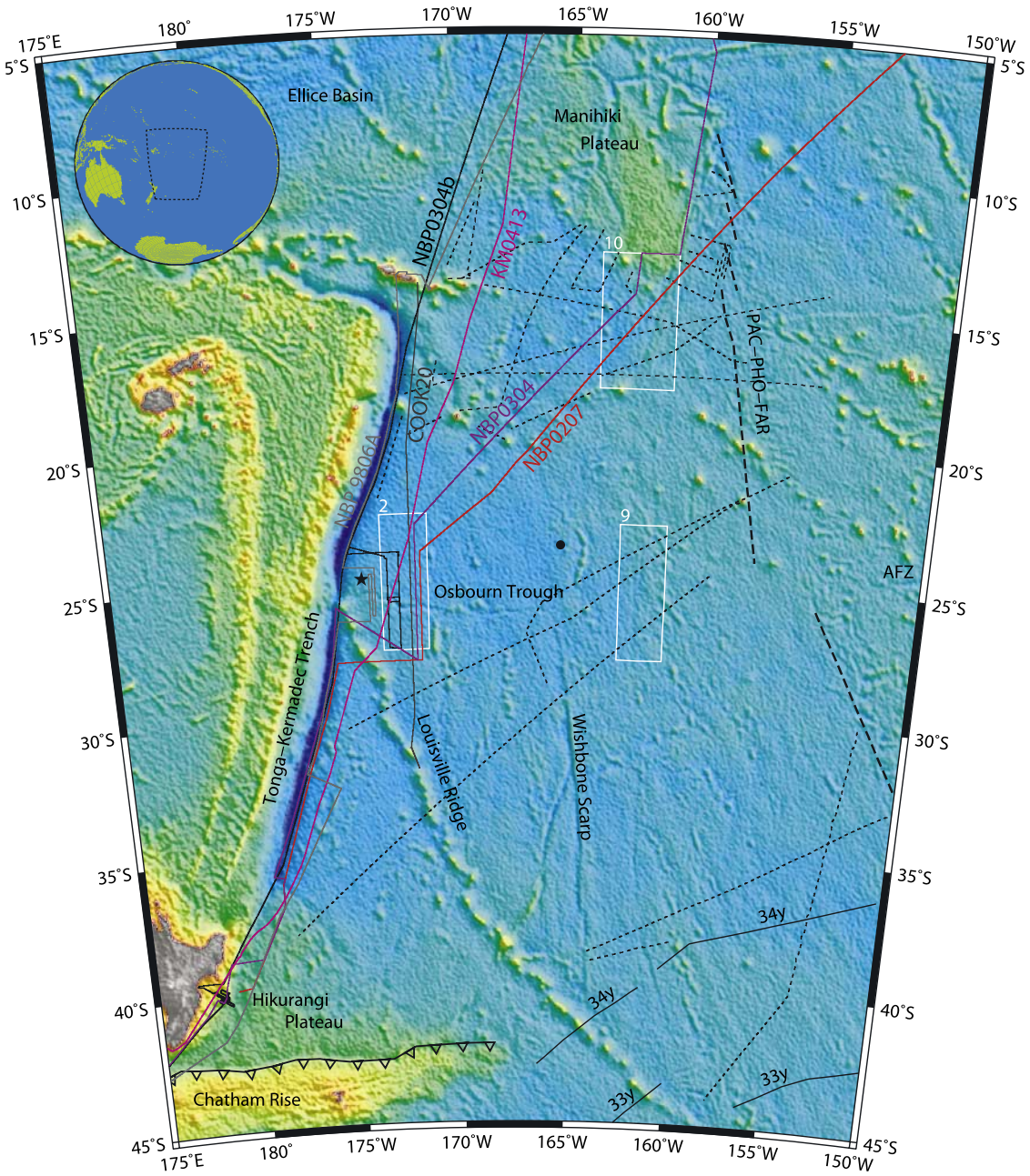

Figure 1. Bathymetric map [*Smith and Sandwell*, 1997] of the Southeast Pacific Basin near the Osbourn region. The locations of the tectonic features discussed in the text are labeled. The location of this figure is shown on the inset globe. The Pacific-Phoenix-Farallon triple junction trace (PAC-PHO-FAR) is plotted as a thick dashed line. The Chatham rise paleosubduction zone is plotted as a line with triangular teeth. The direction of these teeth indicates the direction of paleosubduction. The Osbourn Trough appears as an east-striking bathymetric low near 26°S, the eastern end of which terminates at the intersection with the northern end of the Wishbone Scarp near 165°W. The cruises discussed in the gravity and magnetic data sections are labeled. In addition to these, the sections of multibeam data from several additional cruises analyzed in section 5 are shown as thin dotted lines. The survey geometry provides us the opportunity to study crust created throughout the entire spreading history of the Osbourn spreading center. The locations of Deep Sea Drilling Program sites 205 and 595 are shown as a star and a dot, respectively. At the southern end of the figure the locations of anomalies 34y and 33y on either side of a gravity lineation east of the Wishbone Scarp are plotted as taken from *Larter et al.* [2002]. The differing distance between these anomalies on either side of this lineation demonstrate that it is the location of a paleoplate boundary. The three white boxes labeled 2, 9, and 10 delineate the locations of Figures 2a, 9, and 10, respectively.

with a corresponding early extinction age, or complex plate geometries. A fast spreading rate is expected if the Osbourn Trough is indeed an extinct section of the Pacific-Phoenix ridge as postulated by *Lonsdale* [1997]. This conflict between models results, in part, because the region surrounding the Osbourn Trough formed during the Cretaceous Long Normal Polarity Interval (Chron C34, 121–83 Ma [*Cande and Kent*, 1995]) and therefore lacks the magnetic reversal anomalies useful for determining plate histories. This deficiency has led to the formulation of models based solely on the axial characteristics of the Osbourn Trough, which may only be representative of the last few Ma before the trough's extinction. Confusion also surrounds the origin of several features of the region surrounding the trough. The Wishbone Scarp (Figure 1) is difficult to explain as a fracture zone, as it is very prominent south of the trough but there is no conjugate feature observed in the gravity field north of the trough. Furthermore, the Wishbone Scarp forks to the south, which is not a feature typical of fracture zones. *Mortimer et al.* [2006] assert that the western arm of the Wishbone Scarp is a fracture zone that later became the location of incipient subduction. East of the Wishbone Scarp there is a linear gravity anomaly that is the northern extension of a triple junction trace (Figure 1). The identification of this feature as a triple junction trace is based on the differing distances between Chrons C34y and C33y on either side of this gravity lineation. The reconstruction of *Eagles et al.* [2004] shows this triple junction separated the Phoenix, Pacific, and Charcot plates during the early Cretaceous.

[5] The first extensive marine survey of the Osbourn Trough was carried out aboard the United States Antarctic Program's Research Vessel Icebreaker (*R/VIB*) *Nathaniel B. Palmer* (cruise NBP9806 [*Billen and Stock*, 2000]). Magnetic anomalies were interpreted to indicate that the Osbourn Trough ceased spreading at 71 or 83 Ma [*Billen and Stock*, 2000]. Assuming that rifting between the Manihiki and Hikurangi plateaus began shortly after their formation at the beginning of Chron C34 (121 Ma), *Billen and Stock* [2000] estimated an average full spreading rate (FSR) for the Osbourn paleospreading center of 6–8 cm/yr. This spreading rate is consistent with the trough's morphology, as imaged by multibeam bathymetry. The model proposed by *Billen and Stock* [2000] is similar to that originally proposed by *Lonsdale* [1997] except that he calculated a 15 cm/yr full spreading rate based on a 105 Ma extinction age. This extinction age was hypothesized to correspond to the time when the Hikurangi plateau collided with the Gondwana margin.

[6] *Sutherland and Hollis* [2001] estimate that the crust at DSDP site 595A (Figure 1) formed at 132–144 Ma based on the biostratigraphy of the deepest sediments cored. They use these estimates in conjunction with the observations of *Billen and Stock* [2000] and the 63°S paleolatitude of creation of the crust [*Menard et al.*, 1987] to propose a different model of the history of the Osbourn spreading center. In this model, *Sutherland and Hollis* [2001] propose that two spreading centers were active in this region prior to 120 Ma, the Pacific-Phoenix spreading center and a spreading center to the south separating the Phoenix plate from a newly inferred plate, which they dub the Moa Plate. *Sutherland and Hollis* [2001] propose that the crust at DSDP site 595 was created at the Phoenix-Moa ridge at ca. 137 Ma. After eruption of the Manihiki and Hikurangi plateaus spreading continued on the Phoenix-Moa ridge, which separated the two plateaus. The Osbourn Trough is interpreted to be the extinct western section of this ridge. In order to explain the close proximity of the Osbourn Trough and DSDP site 595, *Sutherland and Hollis* [2001] argue that the East Wishbone Scarp is the remnant of a transform fault that offset the Phoenix-Moa ridge, implying a ~50 Ma age discontinuity at a fracture zone west of DSDP site 595.

[7] Recently, as data from the regions surrounding the Osbourn Trough became more available, tectonic models of these regions have been formulated. These models provide a regional framework into which any tectonic model of the Osbourn Trough must fit. *Larson et al.* [2002] provide a constraint on the location of the Pacific-Phoenix-Farallon triple junction (PAC-PHO-FAR, Figure 1) throughout Chron C34 by examining the changes in abyssal-hill fabric east of the Osbourn Trough. The geometry of this triple junction, along with the area of seafloor created during Chron C34 implies that spreading at the Pacific-Phoenix ridge occurred at 18–20 cm/yr FSR. They also show a change in spreading direction at the Pacific-Phoenix spreading center. Prior to ~100 Ma spreading occurred along an azimuth of ~171°, whereas the spreading direction in regions created after 100 Ma averaged ~164°.

[8] *Eagles et al.* [2004] present a detailed high-resolution reconstruction of the Pacific-Antarctic ridge and associated plate kinematics from 90 to 45 Ma. The earliest part of this reconstruction presents a model of the region south of the Osbourn Trough that provides a late-stage boundary for models of the Osbourn region. *Eagles et al.* [2004] also argue that the spreading directions observed by *Larson et al.* [2002] cannot explain the east-west offset of the Hikurangi and Manihiki plateaus.

[9] *Taylor* [2006] presents a model of the Ellice Basin, a region west of the Manihiki Plateau (Figure 1). This model shows that the Manihiki and Hikurangi Plateaus were not only conjugate to each other at the time of formation but that they were also conjugate to the Ontong Java Plateau. This single large plateau fragmented into at least three parts around 119–123 Ma. *Taylor*'s [2006] model thus provides an early boundary condition for models of the Osbourn spreading center.

[10] *Mortimer et al.*'s [2006] model of the history of the western arm of the Wishbone Scarp asserts that this scarp formed as a fracture zone prior to 115 Ma, was later the location of oblique convergence resulting in the formation of an intraoceanic subduction zone at ca. 115 Ma, and evolved into a rift margin at 92–98 Ma before becoming tectonically inactive. These results constrain the age of the formation of the Osbourn paleospreading center to before 115 Ma. Because the West Wishbone Scarp would have been in close proximity to the Manihiki and Hikurangi plateaus at this time, the observations of *Mortimer et al.* [2006] provide an important constraint on the early history of the Osbourn spreading center.

[11] Ideally, a model of the Osbourn spreading center should be compatible with the history of the Pacific-Phoenix-Farallon triple junction [*Larson et al.*, 2002], provide temporal and spatial continuity between the models of *Taylor* [2006] and *Eagles et al.* [2004] and be consistent

with the observations of *Mortimer et al.* [2006]. A crucial observation for constraining the timing of this model is the age of the crust at DSDP sites 595 and 596 (Figure 1). $^{40}Ar/^{39}Ar$ analyses of the crust cored at site 595/6 yield a minimum age of 100 Ma [*Menard et al.*, 1987]. This estimate is compatible with the 132-144 Ma age of the radiolaria found in the basal sediments (9 m above basement) of hole 595A [*Sutherland and Hollis*, 2001]. However, the radiolarian fossils in the deepest sediments cored at hole 595 (1.5 m above basement) indicate an age of 94–99 Ma.

[12] In this paper we present a new set of ship track surveys of the Osbourn region. These data represent the most extensive survey of the Osbourn Trough thus far and include data collected northward to the Manihiki Plateau (Figure 1). This data set offers us the opportunity to examine regions created continuously at the Osbourn spreading center from its formation to its extinction. We analyze and interpret these data and formulate a new tectonic model that is compatible with the regional tectonics of the Southwest Pacific Basin. We find that contrary to the models of *Billen and Stock* [2000] spreading at the Osbourn spreading center ceased prior to the end of Chron 34. This earlier extinction age matches the models of *Eagles et al.* [2004]. The reduction of the Osbourn spreading center's spreading rate as it approached extinction may be typical of ridge extinction events. This change in spreading rate explains the axial morphology of the Osbourn Trough. We also observe a change in spreading direction throughout the period of active spreading at the Osbourn Trough, which accounts for the east-west offset of the Manihiki and Hikurangi plateaus [*Eagles et al.*, 2004]. Furthermore abyssal hill trends imply that the Osbourn Trough is not an extinct section of the Pacific-Phoenix ridge and therefore that the region of seafloor containing the Hikurangi plateau must have formed a plate separate from the Phoenix plate during the active period of the Osbourn spreading center.

2. Data

[13] We used ship track gravity, magnetic, and seismic data obtained during five separate cruises in this study (Figure 1). Three of these cruises were aboard the *R/VIB Nathaniel B. Palmer*. Two of these *Palmer* cruises (NBP0304 and NBP0207) were transits, only crossing the Osbourn Trough once, while the third (NBP0304b) carried out an extensive survey at a right-stepping offset in the Trough located near 172.7°W. One cruise (KM0413) was a transit carried out aboard the University of Hawaii's School of Ocean and Earth Science and Technology's (SOEST) Research Vessel *R/V Kilo Moana*. The fifth cruise (COOK20) was a transit aboard the Scripps Institution of Oceanography's Research Vessel *R/V Melville*. We also use magnetic anomaly data collected during NBP9806 (Figure 1) [*Billen and Stock*, 2000].

[14] During all five cruises, magnetic field strength and multibeam bathymetry were collected. Swath width of the multibeam surveys averages ~15–20 km for the 4000–6000 m water depths typical of this region of the Southwest Pacific Basin. The processed multibeam data obtained near the Osbourn Trough are shown in Figure 2 superimposed upon bathymetry predicted from satellite altimetry [*Smith and Sandwell*, 1997]. Profiles of the magnetic field strength recorded during our cruises, along with those of NBP9806A [*Billen and Stock*, 2000] are plotted in Figure 3a. Plotted in Figure 3b are the observed magnetic field strength data after being reduced to the pole (skewness = 60°).

[15] In addition gravity data were collected during the three *Palmer* cruises and COOK20. These data are plotted in Figure 4, superimposed upon a series of north-south profiles taken from a global satellite data set [*Sandwell and Smith*, 1997]. There is good agreement between the satellite data and the data collected during the three easternmost cruises. A gravimeter malfunction that occurred during NBP0304b may explain the poor agreement of the satellite data with the NBP0304b ship track data.

[16] Single channel seismic (SCS) data were collected during NBP0207 between latitudes 27°S and 25°S; during NBP0304b, a multichannel seismic (MCS) survey was carried out at the locations shown in Figure 2. The SCS survey carried out during NBP0207 utilized two GI guns with a 3.71 liter capacity, capable of producing energy up to 150 Hz. Ship speed during this survey was 11.1 km/h, with a shot spacing of 37 m. The NBP0304b MCS survey consisted of two north-south lines flanking the 172.7°W offset in the Osbourn Trough and two short east-west lines that cross this offset. A much larger airgun source was used during this survey to image subcrustal structure beneath the Osbourn Trough. A 6 Bolt airgun array with a 34.8 liter total capacity and a shot spacing of 47 m was used for a source. Forty-five channels of data were recorded with a group spacing of 25 m. The seismic data exhibit a two-reflector signature on all seismic lines collected. The uppermost reflector is the seafloor, while the lower reflector 0.0–0.2 s beneath is the sediment-basement contact. Despite the large source sizes used and high number of channels during NBP0304b, no structures are resolved below the sediments.

3. Magnetic Anomalies

[17] The magnetic field strength profiles of Figure 3a are shifted such that they are aligned along the axis of the Osbourn Trough. If the observed anomalies are due to magnetic field reversals, there should be a correlation among all the profiles. However, the magnetic field strength profiles adjacent to each other correlate better than those far apart. In particular, NBP0304 correlates better with both NBP0207 and COOK20 (correlation coefficient, R = 0.65 and 0.79, respectively) than it does with either of the west

Figure 2. (a) Multibeam data collected near the Osbourn Trough during our cruises, superimposed upon predicted bathymetry from satellite altimetry [*Smith and Sandwell*, 1997]. The locations of the NBP0207 SCS and NBP304b MCS surveys are shown by the locations of the red and black dashed lines, respectively. The white box outlines the location of Figure 2b. (b) Close-up of Figure 2a highlighting the change in abyssal-hill character that occurs between 24°S and 25°S. The abyssal-hill fabric north of 24.5°S is much smoother than the fabric south of 24.5°S. This change in texture is not accompanied by a change in sediment thickness, so the subdued fabric to the north cannot result from sediment smoothing.

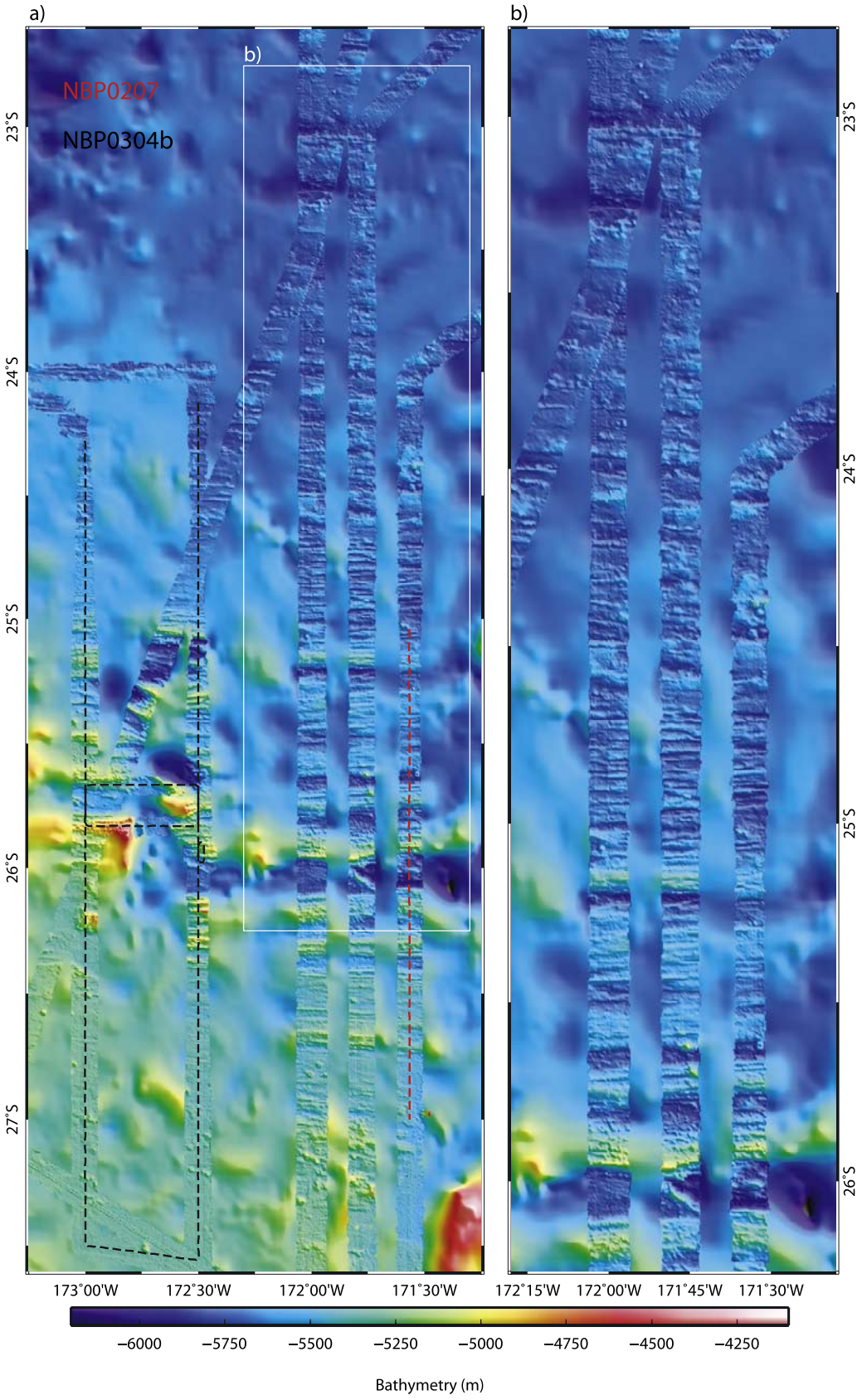
a)
b)
NBP0207
NBP0304b
23°S
24°S
25°S
26°S
27°S
173°00'W
172°30'W
172°00'W
171°30'W
b)
23°S
24°S
25°S
26°S
172°15'W
172°00'W
171°45'W
171°30'W
−6000
−5750
−5500
−5250
−5000
−4750
−4500
−4250
Bathymetry (m)

Figure 2

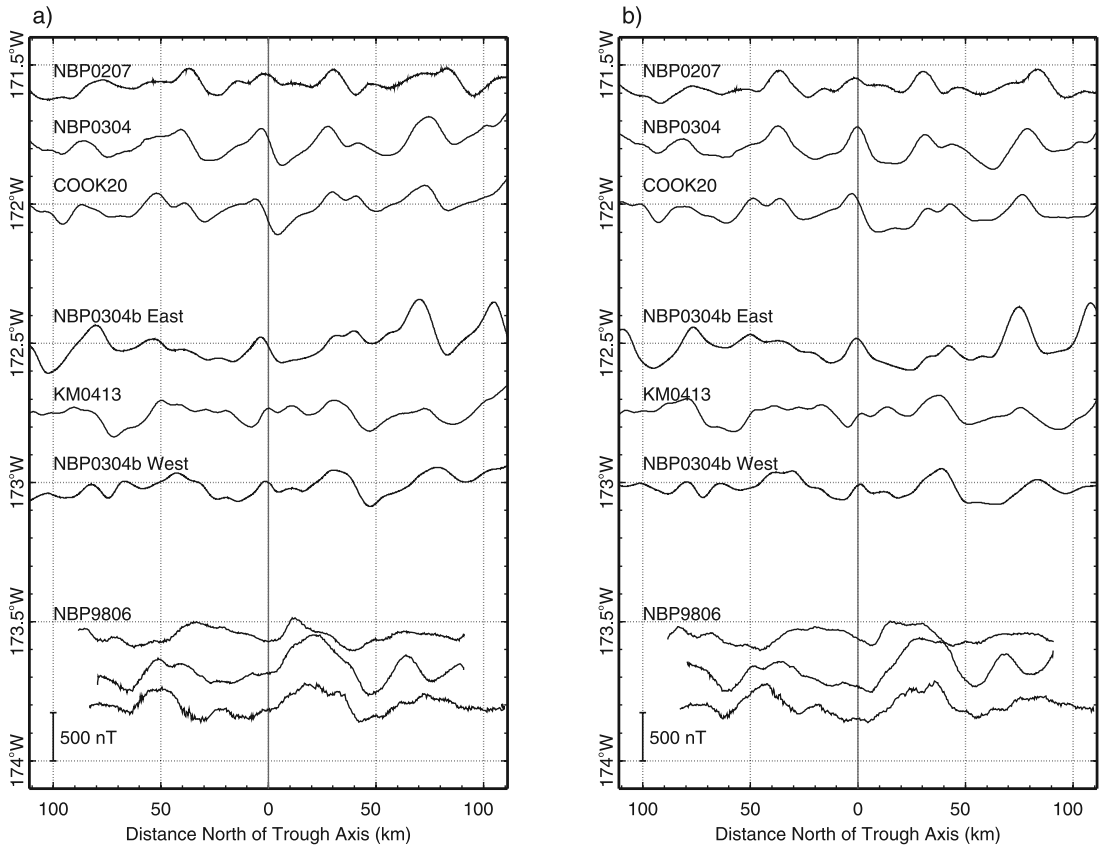

Figure 3. (a) Magnetic anomaly data observed at the Osbourn Trough. The magnetic profiles have been aligned along the axis of the Osbourn Trough (the trough axis coincides with the central solid vertical gridline). Included in this figure are our data along with that of a previous survey, NBP9806 [*Billen and Stock*, 2000]. The lack of correlation across the survey area indicates that the magnetic anomalies cannot result from magnetic field reversals. (b) Magnetic anomaly data in Figure 3a after application of a reduction to the pole filter (skewness = 60°). The symmetry of the phase-shifted profiles shows that these anomalies may result from fluctuations in the magnetic field strength during Chron C34. Similar fluctuations have been observed to occur during Chron C5 [*Bowers et al.*, 2001].

and central profiles of NBP9806 (R = 0.34 and 0.20) even though these two NBP9806 profiles correlate well with each other (R = 0.75). *Billen and Stock* [2000] present models of the NBP9806 profiles that predict either a 71 Ma (preferred) or an 83 Ma extinction age for the Osbourn spreading center. However, because the correlation between the profiles in Figure 3a disappears with increasing distance between profiles, the models of *Billen and Stock* [2000] do not predict the shape of our magnetic anomaly data. The lack of correlation across our survey area indicates that the source of the observed anomalies cannot be magnetic field reversals, casting doubt on the extinction age estimates of *Billen and Stock* [2000] and on paleospreading rates inferred from those estimates.

[18] The phase-shifted profiles (Figure 3b) have a strong symmetry about the axis of the Osbourn Trough indicating that the magnetic anomalies are most likely due to magnetic field strength fluctuations within Chron C34. Similar fluctuations have been observed within Chron C5 [*Bowers et al.*, 2001]. We therefore conclude that the Osbourn spreading center stopped spreading some time during Chron C34 (121–83 Ma); however, the exact extinction age cannot be determined by analysis of the observed magnetic anomalies.

4. Gravity Models

4.1. Spreading Rates From Gravity Measurements

[19] Active spreading centers are generally characterized by a linear residual gravity anomaly coincident with the ridge axis. The shape of this anomaly depends on the ridge's spreading rate [*Small*, 1994; *Watts*, 1982]. A similar pattern is observed in the gravity fields of extinct spreading axes [*Jonas et al.*, 1991].

[20] *Jonas et al.* [1991] interpret the central gravity lows observed at extinct spreading centers as changes in crustal geometry beneath the axial valley. They use this model to successfully explain the residual gravity of several extinct spreading centers. Their model is based on the observation that the basal portions of the oceanic crust emplaced at the Bay of Islands ophiolite complex formed at high pressures within the mantle. *Elthon et al.* [1982] propose a model in which these portions form at a depth of ~30 km beneath the ridge axis, flow upward along an upwelling conduit of

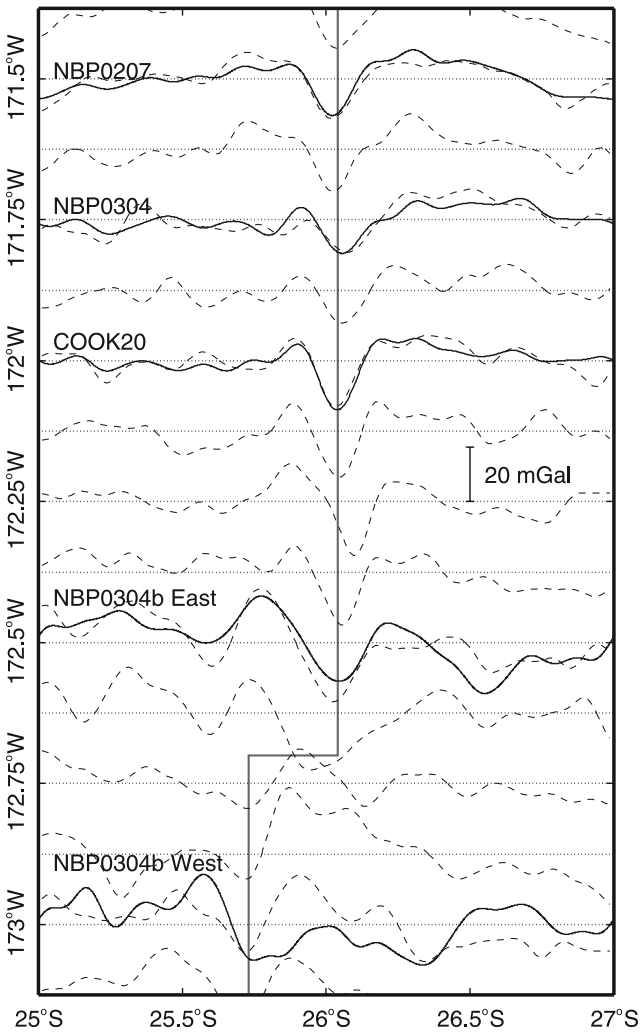

Figure 4. Gravity data observed near the Osbourn Trough after the removal of regional values. Our ship track data are shown as solid lines. The dashed lines are north-south profiles taken from a global gravity data set [*Sandwell and Smith*, 1997]. The straight dotted lines show the zero value for each profile. The solid gray line follows the Osbourn Trough axis. The Osbourn Trough coincides with the gravity lows at 26°S and 25.2°S, east and west of 172.7°W, respectively.

material as the oceanic plates rift apart, and are emplaced at the base of the oceanic crust. *Jonas et al.* [1991] propose that this conduit becomes frozen upon ridge extinction displacing higher-density mantle material resulting in a gravity low. Recently, *Müller et al.* [2005] were able to model the gravity field of the Adare Trough using this Moho topography model.

[21] Seismic reflection and refraction data obtained at the Labrador Sea paleospreading center indicate that crustal thickness decreases toward the ridge axis [*Srivastava and Keen*, 1995]. Magnetic reversal anomalies observed near the ridge axis indicate that the region of reduced crustal thickness (4–6 km versus 6–7 km thick) was formed during a 13 million year period of slower spreading (0.6 cm/yr versus 2 cm/yr) immediately prior to ridge extinction. This crustal thinning is accommodated by extension along numerous faults in the crust of this region and seismic velocities at the axis are anomalously low through the crust and upper 3 km of the mantle [*Srivastava and Keen*, 1995]. *Osler and Louden* [1992] hypothesize that these regions have undergone serpentinization resulting in lower densities and seismic velocities, a process that may have been aided by the presence of several faults that penetrate the crust near the ridge axis. The regions of altered density may be sufficiently large to explain the gravity anomaly observed at the Labrador Sea paleospreading center [*Osler and Louden*, 1992].

[22] *Jung and Vogt* [1997] observe that the crust thins at the axis of the Aegir Ridge, located in the Norwegian Sea, similar to the observations of *Osler and Louden* [1992] at the Labrador Ridge. *Uenzelmann-Neben et al.* [1992] observed a change in the amplitude of sediment-layer reflections at the axis of the Aegir Ridge. This change is due to a change in pore fluids in the sediments of the axial region. Observing that the Aegir Ridge is characterized by a residual gravity low, *Uenzelmann-Neben et al.* [1992] infer that the sediment pore fluids of the axial region were released from a crustal magma chamber as it solidified during its extinction. The residual gravity low at the Aegir Ridge may therefore be due to a low-density region within the crust.

4.2. Osbourn Trough Gravity

[23] The gravity field of the Osbourn Trough is similar to that observed at the Labrador Sea, Aegir Ridge, and other extinct spreading centers. In Figure 4 the axis of the Osbourn Trough coincides with the gravity low centered at 26°S east of 172.5°W. The trough shifts northward west of this point and coincides with a similar gravity low at 25.75°S. In fact the Osbourn Trough is a more prominent feature in gravity data sets than in bathymetric data sets, and it is not surprising that the trough was not originally identified on bathymetric maps but rather was recognized by its axial gravity anomaly [*Lonsdale*, 1997].

[24] The observed gravity profiles (Figure 4) are composed of several components. A 15–20 mGal, 30 km wavelength gravity low centered on the axis of the Osbourn Trough is seen in all shiptrack and satellite profiles. Superimposed upon this, the gravitational expression of abyssal hills correlates with bathymetry and is reflected as 5–10 mGal ~20 km wavelength oscillations present throughout the profiles (compare the seismically determined bathymetry in Figures 5a–5c with the observed gravity). The longest wavelength components of the gravity field could be caused by changes in crustal thickness or large-scale density anomalies located in the mantle. The amplitude of the axial gravity anomaly cannot be explained by bathymetry and sediment cover. *Billen and Stock* [2000] argued that the axial gravity anomaly seen at 173.7°W would require an increased sediment thickness in the trough axis, and they predicted that at this location, to account for the gravity anomaly, sediment cover would have to be 350 m thick. Our seismic data show, however, that sediments in the trough axis at the locations of our seismic surveys (Figure 2) are only 60–70 m thick. Note also that single-channel seismic reflection data obtained during Deep-Sea Drilling Project (DSDP) leg 91 by the drilling vessel *Glomar Challenger* demonstrate that the Osbourn Trough at 26°S

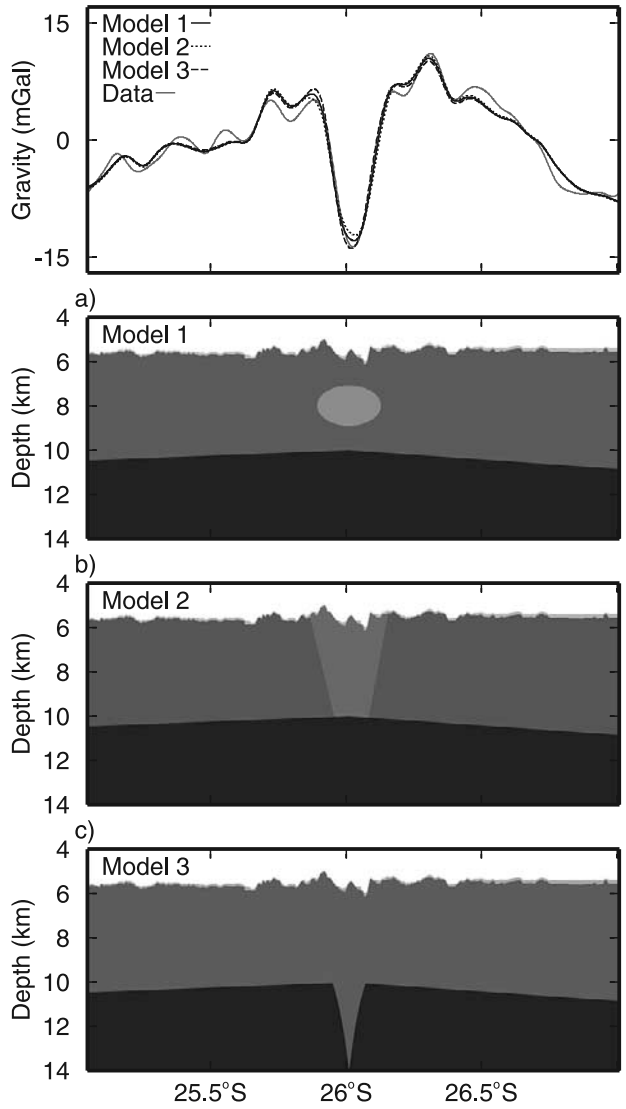

Figure 5. Models of the density structure of the Osbourn Trough that accurately predict the observed data. (a) A single low-density region beneath the trough axis. (b) A low crustal density model where the crust density has been modified by hydrothermal alteration. (c) The Moho topography model of *Jonas et al.* [1991]. Densities for each of these models that provide the best fit to the data are given in Table 1. The output of each of these models (top) fits the data equally well.

169°W is 500 m deep and contains a thin (<70 m) sediment infill [*Menard et al.*, 1987]. The thin sediment infill of the Osbourn Trough implies that the axial anomaly must be due to density anomalies in the crust or uppermost mantle, density anomalies that may be explained by the serpentinization, Moho topography, or low-density crustal body models that have been invoked to explain the gravity anomalies of other extinct spreading centers.

4.3. Gravity Models of the Osbourn Trough

[25] *Nettleton*'s [1939] method of gravity interpretation uses the topography and free air anomaly of a region to determine average subsurface density. This method is valid as long as topography and density do not correlate, such as would occur if the topography were locally compensated. In our analysis we extend *Nettleton*'s [1939] method to more complex models. The model domain is separated into several subdomains each of which has a constant density and represents a particular model element (e.g., sediments, crust, etc.). The gravitational field of each subdomain for a unit density is calculated using *Parker*'s [1972] method. The modeled gravity is given by the equation:

$$g(x) = \sum_{j=1}^{N} \rho_j \varphi_j(x) + b \quad (1)$$

where g(x) is the modeled gravity along the profile, $\varphi_j(x)$ is the unit density gravity field of the jth subdomain, N is the total number of subdomains, b is the average background gravity of the region, and ρ_j is the density of the jth model element. This approach requires us to prescribe only the shape of the model elements; the densities (ρ_j) are determined by a least squares inversion of the measured gravity field. Our method requires nonlocal topographic compensation, and at the wavelengths considered in our model ($\leq$50 km) this requirement is satisfied for typical oceanic regions [*Watts*, 2001].

[26] To incorporate the seismic observations into this modeling process, the water-bottom and sediment-basement interfaces were interpreted from the migrated seismic sections. A time to depth conversion was then carried out using a 1500 m/s velocity for the water column and a 1600 m/s velocity for the sediments, based on measurements at DSDP site 204 [*Burns et al.*, 1973, Figure 2]. This time-depth conversion provides the geometry of the sediment and basement layers in the gravity models.

[27] We have constructed three models that predict the Osbourn Trough's gravity field (Figure 5 and Table 1). Model 1 contains an elliptical low-density body within the crust. A tradeoff exists between the density contrast of this body with the crust and the thickness of this ellipse; however, for a given depth, the width remains fixed regardless of density contrast. The depth of this ellipse can also vary without affecting the calculated densities. Deeper ellipses are narrower than shallow ones.

[28] The limit of a superposition of a large number of ellipses at a range of depths leads to model 2. This model presents low crustal density as the cause of the axial gravity anomaly. The geometry of this low-density zone is well-constrained by the gravity data, assuming that it extends

Table 1. Densities of Gravity Model Elements

	R^2	$\rho_{sediment}$, g/cm^3	ρ_{crust}, g/cm^3	ρ_{mantle}, g/cm^3	ρ_{body}, g/cm^3
Model 1 (Low-Density Body)	0.88	1.61 ± 0.20	2.48 ± 0.04	3.26 ± 0.06	2.04 ± 0.04
Model 2 (Low Crustal Density)	0.87	1.67 ± 0.21	2.52 ± 0.04	3.32 ± 0.06	2.36 ± 0.04
Model 3 (Crustal Root)	0.88	1.77 ± 0.13	2.47 ± 0.13	3.28 ± 0.05	-

from the surface of the crust to the Moho and may result from fracturing or hydrothermal alteration. A depth of alteration greater than or less than the Moho would yield density contrasts between the altered zone and normal crust less than or greater than those in Table 1, respectively.

[29] Our third model is based upon the model of *Jonas et al.* [1991], with the gravity signature of the Osbourn Trough resulting from the geometry of the Moho alone; no low-density anomaly within the crust is required. There is a tradeoff between the width and depth extent of the crustal root. If the root extends to 30 km deep, as postulated by *Jonas et al.* [1991], it would become a conduit only a few kilometers wide.

[30] These three models may be overly simplistic, but they are a useful starting point for examining the gravity anomalies. We have assumed constant density within each model element but our method is insensitive to vertical density gradients. Models that contain such gradients and also preserve the density contrasts between elements produce identical results. Each of our three models explains observations equally well and yields densities for their common elements (crust, mantle, and sediments) that are similar (Table 1).

[31] Our gravity models do not allow us to draw unique conclusions about the density structure of the Osbourn Trough. They do, however, show that the gravity field of the Osbourn Trough is typical of that at other extinct spreading axes. Furthermore, the amplitude of the axial anomaly is similar to that observed at the axes of extinct ridges with ~5.5 cm/yr full paleospreading rate [*Jonas et al.*, 1991]. This estimate provides an important constraint on the history of the Osbourn spreading center immediately prior to extinction.

5. Abyssal-Hill Fabric

5.1. Spreading Rate and Direction From Abyssal Hill Fabric

[32] Abyssal hills are elongate ridges on the ocean floor whose shape varies by region [*Goff and Jordan*, 1988; *Hayes and Kane*, 1991; *Menard*, 1967]. They are created at spreading centers and form the uppermost layer of oceanic crust and, postcreation, form a series of flanking ridges whose long axis parallels the spreading center. The primary control on abyssal-hill morphology is faulting, which occurs at mid-ocean ridges shortly after crustal formation [*Buck and Polikov*, 1998; *Goff et al.*, 1995; *Macdonald et al.*, 1996]. This faulting process is controlled by the stress state at the ridge, leading to a correlation between abyssal-hill shape and ridge characteristics [*Goff*, 1991; *Goff et al.*, 1997; *Kriner et al.*, 2006]. These characteristics include spreading rate, spreading direction, and ridge axial-valley morphology. Thus evaluating abyssal-hill morphology makes it possible to reconstruct the tectonic history of a region in the absence of magnetic reversal anomalies [*Menard*, 1967]. It is not possible, however, to directly determine seafloor ages from abyssal-hill morphology, making it necessary to infer ages from other data types (e.g., biostratigraphy and isotopic dating of core or dredge samples) in regions devoid of magnetic reversal anomalies.

[33] During their creation, the long axes of abyssal hills preferentially align with the trend of the ridge; therefore because spreading is generally perpendicular to the ridge axis, the direction normal to abyssal-hill strike is an indicator of paleospreading direction. The alignment of abyssal hills is not perfect, however, and some scatter of azimuths is observed within regions created at a single spreading center. This scatter makes is necessary to define regions of relatively constant trend over which a single estimate of abyssal hill trend can be made. By observing where abyssal-hill trends change from generally north-south to east-west, *Larson et al.* [2002] were able to determine the spreading directions of the Pacific-Phoenix and Pacific-Farallon spreading centers during Chron C34.

[34] *Menard* [1967] observed that the root-mean-square (RMS) amplitude of abyssal hills negatively correlates with the spreading rate of the parent ridge during abyssal-hill formation. Later studies [*Goff*, 1991; *Goff et al.*, 1997; *Hayes and Kane*, 1991] confirm this correlation for slow spreading ridges with RMS amplitudes varying from ~220 m for regions created at ridges with a full spreading-rate (FSR) of 2 cm/yr, to ~60 m for regions created at ridges with spreading at 7 cm/yr FSR. *Goff et al.* [1997] find that this correlation breaks down for areas formed by ridges spreading faster than 7 cm/yr. Faster-spreading (>7 cm/yr FSR) ridges produce seafloor whose RMS amplitude is 50–60 m and independent of spreading rate.

[35] Abyssal-hill width is defined as the horizontal scale of abyssal hills measured perpendicular to the hill's azimuth. *Goff*, [1991, 1997] observe that as abyssal hills get higher they also get wider. As a result, there is also a correlation between abyssal-hill width and the spreading rate of the parent spreading center during abyssal-hill formation. The characteristic width of abyssal hills decreases from ~8 km for crust created at 2 cm/yr FSR to ~2 km for crust created at 7 cm/yr FSR. Characteristic width increases with increasing spreading rate for faster rates, from 2 km at 7 cm/yr FSR to 3 km for crust created at 16 cm/yr FSR. *Goff*, [1991] attribute this increase to the complex spreading histories typical of extremely fast spreading ridges.

[36] The degree of abyssal hill asymmetry, defined as the difference in slope magnitude between the inward facing (toward the spreading axis) and outward facing sides of an abyssal hill, also correlates with spreading rate [*Kriner et al.*, 2006]. Unlike the correlations between abyssal-hill width and spreading rate and between abyssal-hill RMS amplitude and spreading rate, the correlation between abyssal-hill asymmetry and spreading rate does not change at the transition between axial-valley and axial-high morphology at ~7 cm/yr FSR.

5.2. Osbourn Trough Abyssal-Hill Morphology

[37] We hope to answer the following two questions by analyzing the abyssal-hill fabric observed near the Osbourn Trough: (1) Was there ever an east-west component of spreading on the Osbourn spreading center that can explain the east-west offset of the Manihiki and Hikurangi plateaus? (2) Was there a change in spreading rate prior to the extinction of the Osbourn spreading center and if so, how does that change the inferred extinction age for the Osbourn spreading center?

[38] Our surveys are ideal for this type of analysis because they extend away from the trough for several

hundred kilometers. Two surveys (those conducted during NBP0304 and NBP0207) extend northward to the Manihiki plateau, providing a record of abyssal hills generated at the Osbourn spreading center throughout its entire active period. In addition to the labeled ship tracks in Figure 1, we also analyze abyssal hill trends observed in several other multibeam surveys (dotted lines in Figure 1). These additional surveys provide continuous coverage between regions created at the Osbourn spreading center and the regions created at the Pacific-Phoenix ridge, discussed by *Larson et al.* [2002].

[39] The location of changes in abyssal-hill morphology cannot be identified a priori so we use a technique of parameter estimation that is spatially local to define regions of relatively constant abyssal-hill properties. For abyssal-hill trends a single estimate of paleospreading direction is then made for each region.

[40] In this paper we estimate abyssal-hill statistics by the application of a ridgelet transform method to the multibeam bathymetry data [*Downey and Clayton*, 2007]. This method utilizes the ridgelet transform of *Candès* [1998] and *Candès and Donoho* [1999] to locally estimate abyssal-hill azimuth, width, and RMS amplitude. An issue that arises in the use of abyssal fabric is the effect of erosion and sedimentation on the estimates. Fortunately, seismic data are available to allow us to quantify this effect. In Appendix A we discuss the effect of sedimentation on abyssal-hill parameter estimates.

[41] Application of the ridgelet transform procedure to our multibeam data shows that the abyssal hills observed north and south of the Osbourn Trough can be divided into four groups based on azimuth trends and location (Figure 6). The first group, designated the ''Manihiki'' abyssal hills, consists of the abyssal hills observed between the southern side of the Manihiki Plateau and 22°S. The mean azimuth of this population is 104.7° ± 1.7° (95% confidence interval; Figure 6). The second group, the ''North Osbourn'' abyssal hills in Figure 6, consists of the abyssal hills observed between 22°S and the axis of the Osbourn Trough at 26°S. These abyssal hills have a mean azimuth of 92.1° ± 3.1°, and the results of a Watson-Williams test [*Zar*, 1999] show that this group has a different mean from the Manihiki abyssal hills with 95% confidence. Further subdivision of the observed azimuths into smaller populations does not yield any populations with average azimuths intermediate to those of the Manihiki and North Osbourn abyssal hills. South of the Osbourn Trough a similar pattern is observed. The ''South Osbourn'' abyssal hills, those observed between 30°S and the Osbourn Trough, have a mean azimuth of 94.8° ± 3.5°, similar to the mean azimuth of the North Osbourn abyssal hills. South of 30°S the fourth group, the ''Hikurangi'' abyssal hills, have mean trend of 110.1° ± 7.3° which likewise is similar to the azimuth of the Manihiki abyssal hills. Like the Manihiki and North Osbourn Abyssal hills, the two groups south of the Osbourn Trough also have differing means at a 95% confidence level. However, the sharpness of the transitions at 22°S and 30°S cannot be accurately determined from our data. We estimate that the locations of these transitions are accurate to approximately 1°. The symmetric pattern of abyssal-hill azimuths about the Osbourn Trough is in agreement with the spreading center origin of the Osbourn Trough. The change in abyssal-hill azimuth indicates that the spreading direction of the Osbourn paleospreading center changed from an azimuth of ~13.0° to ~2.8° at the time when the crust near 22°S and 30°S was simultaneously being created.

[42] Two groups of abyssal hills east of those created at the Osbourn Trough are also shown in Figure 6. These populations are those described by *Larson et al.* [2002] as being created at the Pacific-Phoenix spreading center during Chron C34. North of the Austral Fracture Zone (AFZ; Figure 1) we observe the ''North PAC-PHO'' abyssal hills, whose mean azimuth is 78.4° ± 6.5°. South of the AFZ are the ''South PAC-PHO'' abyssal hills, which have mean azimuth 74.1° ± 3.5°. Both of these populations have means that are different from the four Osbourn abyssal hill groups as well as from each other at a 95% confidence level.

[43] The output of the RMS amplitude and width analysis of the abyssal hills created at the Osbourn spreading center is shown in Figures 7 and 8, respectively. These two statistics are influenced by sediment cover, so we restrict our analysis to the ship tracks near the western end of the Osbourn Trough where sediments are thinnest and where we have seismic data constraints on sediment thickness. The results of this analysis are shown for latitudes between 26°S and 20°S. North and south of these latitudes, thick sediments blanket the abyssal-hill fabric, casting doubt on our estimates of the abyssal-hill RMS amplitude and width (see Appendix A). Similarly, ship tracks approaching the Tonga-Kermadec subduction zone pass into terrain faulted by extension related to subduction. We have also avoided the region of anomalous bathymetry north of the 172.7°W trough offset (i.e., a ''discordant zone'' [*Macdonald et al.*, 1991]). In the locations presented in Figures 7 and 8 our estimates of abyssal-hill width and amplitude are believed to be representative of the basement topography created at the Osbourn spreading center. The RMS amplitude of the bathymetry decreases from 250 to 300 m at the trough axis near 26°S to 50 m north of 25°S (Figure 7). The RMS amplitude north of 25°S is approximately 50–60 m for all ship tracks northward until latitude 23.3°S. North of this point the RMS amplitudes begin to fluctuate about 50 m with a maximum excursion of ~110 m and a minimum of ~25 m. The largest excursions occur in regions of increasing

Figure 6. Abyssal-hill azimuths as determined via ridgelet transform. The azimuth estimates have been split into six populations, the Manihiki, North Osbourn, South Osbourn, and Hikurangi abyssal hills, all of which were created at the Osbourn spreading center, and the North and South Pacific-Phoenix abyssal hills. A rose diagram of each population is shown. The size of each population is presented along with the mean azimuth and 95% confidence interval. The difference between the strikes of the Manihiki/Hikurangi populations and the Osbourn abyssal hill populations indicates a change of spreading direction at the Osbourn spreading center. Furthermore, the difference between the Osbourn and Pacific-Phoenix abyssal hills indicates that the Osbourn spreading center was not a section of the Cretaceous Pacific-Phoenix ridge.

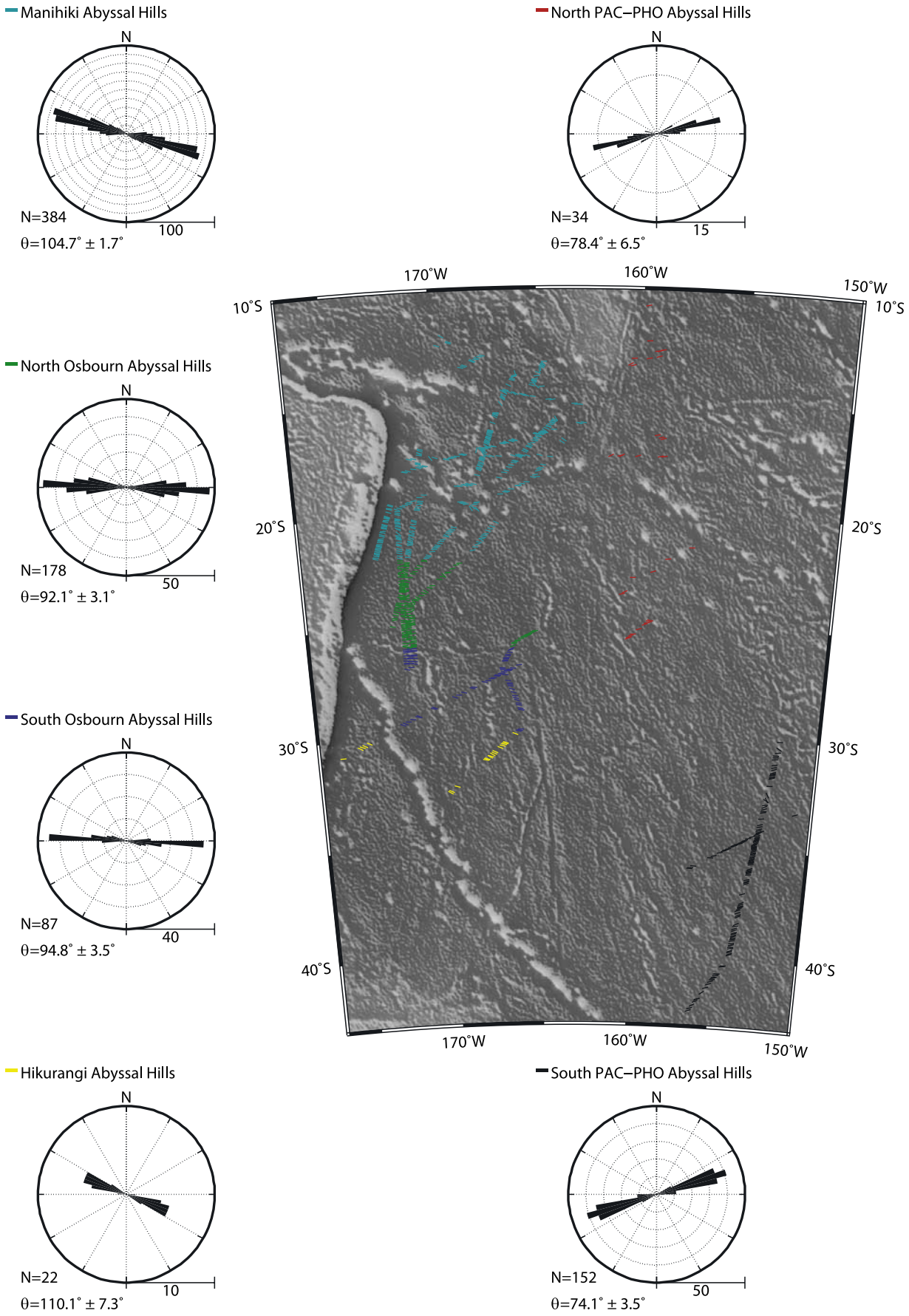
Manihiki Abyssal Hills
N
N=384
100
θ=104.7° ± 1.7°
North PAC–PHO Abyssal Hills
N
N=34
15
θ=78.4° ± 6.5°
170°W
160°W
150°W
10°S
20°S
30°S
40°S
North Osbourn Abyssal Hills
N
N=178
50
θ=92.1° ± 3.1°
South Osbourn Abyssal Hills
N
N=87
40
θ=94.8° ± 3.5°
Hikurangi Abyssal Hills
N
N=22
10
θ=110.1° ± 7.3°
South PAC–PHO Abyssal Hills
N
N=152
50
θ=74.1° ± 3.5°

Figure 6

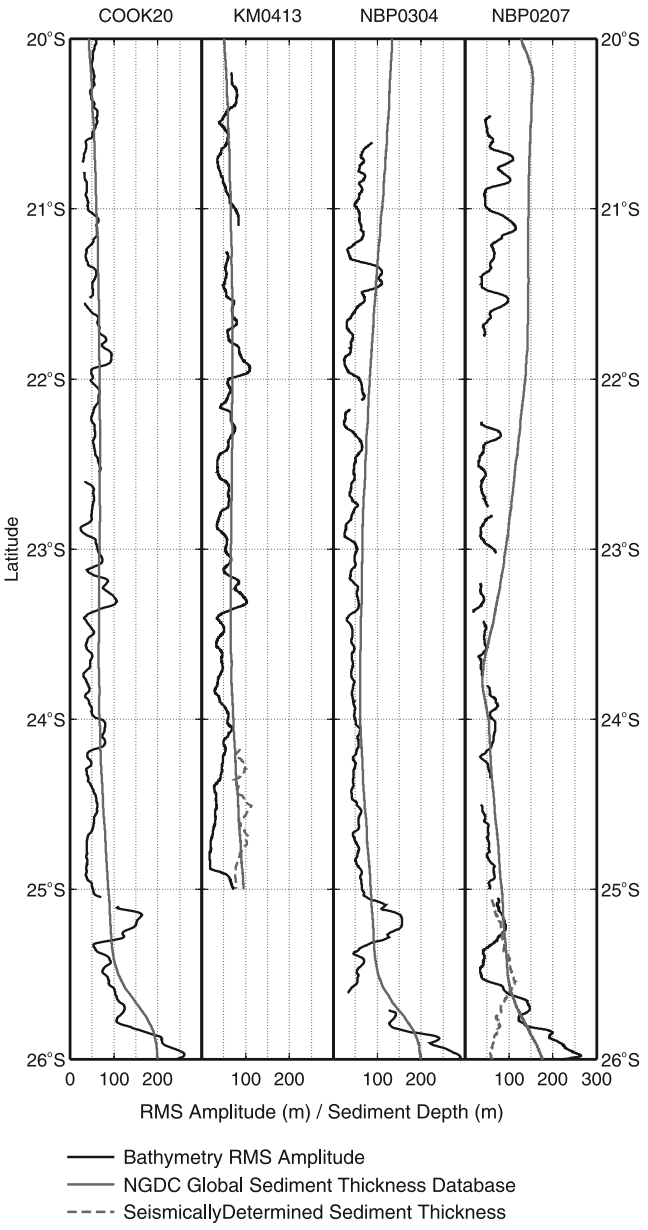

Figure 7. Abyssal hill RMS amplitude for regions not contaminated by seamounts or thick sediments. The solid gray lines show sediment depth along each ship track taken from the NGDC global sediment database. The solid black lines are the RMS amplitude of bathymetry calculated along the profiles. RMS amplitude increases greatly south of 25°S. North of this latitude it remains relatively stable at 50–60 m, with some fluctuations occurring as sediments get thicker. The gray dashed line in the NBP0207 panel denotes the sediment thickness interpreted from the NBP0207 SCS data. The agreement between this thickness estimate and the NGDC database is closest northward, away from the Osbourn Trough. The KM0413 data are presented north of 25°s, as south of this latitude KM0413 passes into the ''discordant zone'' associated with an offset in the Osbourn Trough. The results are also similar with very smooth bathymetry being observed northward to 20°S. The gray dashed line in the KM0413 figure is the sediment thickness at the northern end of the eastern NBP0304b MCS line (see Figure 2 for location).

sediment thickness at the northern ends of NBP0207 and NBP0304 (grey curves in Figure 7).

[44] The general trend north of 25°S is that where sediments are thin (<80 m thick) RMS amplitudes are small, approximately 40–70 m with a few excursions to 100 m. The results of *Goff et al.* [1997] and *Hayes and Kane* [1991] allow us to estimate spreading rates for the region of our analysis. The decrease in RMS amplitude from 250 m to 50 m between 26°S and 25°S corresponds to a drop in spreading rate from >7 cm/yr FSR at the time of formation of the crust at 25°S to 2 cm/yr FSR immediately prior to extinction of the Osbourn spreading center. The region north of 25°S where RMS amplitude is 50–70 m corresponds to formation at spreading rates >7 cm/yr FSR. Unfortunately, as discussed above, we cannot constrain the exact spreading rate for this region as the correlation between RMS amplitude and spreading rate only holds for rates less than 7 cm/yr FSR.

[45] The widths of abyssal hills in this region also vary (Figure 8). Between 24.5°S and 26°S widths range from 1.5 to 16 km. North of 24.5°S the smallest scales are subdued with widths generally ranging from 2 to 16 km. Abyssal-hill widths less than 2 km correspond to a spreading rate of ~8 cm/yr FSR [*Goff et al.*, 1997]. The smaller widths at the trough axis may be explained by increased faulting near the axis of the Osbourn spreading center during the last few million years of spreading. Increased faulting immediately prior to the extinction of the Labrador ridge was observed by *Srivastava and Keen* [1995].

[46] It is difficult to use abyssal-hill widths to constrain the spreading rate of the Osbourn spreading center because we observe a wide range of scales in all regions of our survey and are unable to designate any particular width as dominant (Figure 8). Furthermore, as increasing sediment thickness obscures the finest scales first, the true range of scales may be even larger than what we observe. This wide range of observed scales is interesting in itself as it indicates that the faulting process that forms abyssal hills can create them at several scales simultaneously.

[47] The abyssal hill analysis yields some important constraints on the tectonic history of the Osbourn spreading center. When the Hikurangi and Manihiki Plateaus rifted, the subsequent spreading that continued to separate the two plateaus took place along a 15°–20° azimuth. The east-west component of this spreading may explain the modern east-west offset of the Hikurangi and Manihiki plateaus. At some point prior to extinction the spreading direction at the Osbourn spreading center changed relatively suddenly to an azimuth of 2°–5° ~450 km from the modern trough axis. We also know that the spreading rate slowed significantly immediately prior to the extinction of the spreading center. If the last 110 km of the crust north and south of the trough was emplaced at an average full spreading rate of 2–6 cm/yr (a range that is in agreement with RMS amplitudes, gravity, and morphology observed at the trough axis), then this slowing began 2–6 Ma before ridge extinction. The RMS amplitude of bathymetry also indicates that prior to this slowing the spreading rate was >7 cm/yr FSR. In order to better constrain this spreading rate and determine the timing of the events outlined by the abyssal-hill strikes we must combine our results with other data obtained near the Osbourn region.

[48] Two additional features of interest in the bathymetry of the Osbourn region are shown in Figures 9 and 10. The region in Figure 9, east of the Wishbone Scarp contains two long linear features (highlighted with dashed lines) that may be the bathymetric expression of fracture zones. These two features are subparallel to and located between the Southeast Manihiki Scarp and the triple junction trace described by *Eagles et al.* [2004, Figure 1]. However, we are unable to determine if these features are connected to either the triple junction trace or the Southeast Manihiki Scarp due to a lack of data north and south of these lineations. Several short lines delineate a series of ridges observed southwest of the Manihiki Plateau in Figure 10. These ridges are isolated to this region and their trend parallels neither the local abyssal hill fabric nor the trend of the Southeast Manihiki Scarp. These ridges may result from the rifting event that first separated the Manihiki and Hikurangi plateaus as they are approximately parallel to the trend of the southwest margin of the Manihiki Plateau.

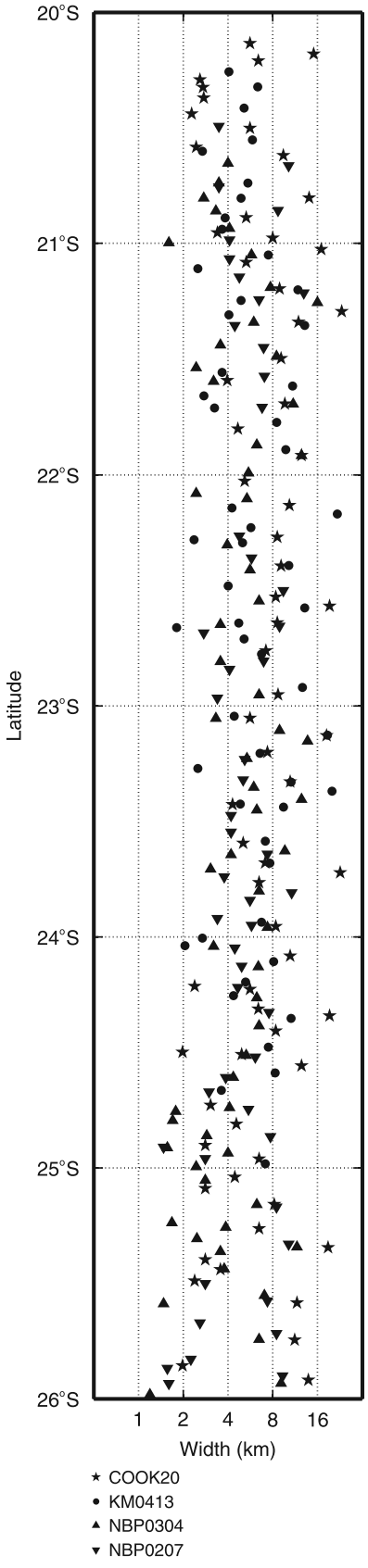

Figure 8. Widths of abyssal hills as determined via ridgelet transform. All cruises display similar behavior, with no particular scale being dominant for any latitude band. There is an increase in small-width abyssal hills near the Osbourn Trough axis at 26°S. These small scales may result from increased faulting near the axis. This figure demonstrates that the process that creates abyssal hills at trough axes does so at a variety of scales simultaneously.

6. Tectonic Model

6.1. Geometry of Osbourn Spreading

[49] Abyssal-hill strikes provide constraints on the geometry of spreading at the Osbourn spreading center. Spreading initially occurred at an azimuth of approximately 15°–20°, based on the trends of the Hikurangi and Manihiki abyssal hills, but later rotated to a 2°–5° azimuth as indicated by the near east-west strike of the abyssal hills that flank the Osbourn Trough. On the basis of these constraints we have formulated a geometrical model of spreading at the Osbourn paleospreading center (Figure 11).

[50] Figure 11a shows the initial configuration of the Manihiki and Hikurangi Plateaus immediately prior to their separation. This configuration matches that proposed by *Taylor* [2006] and predates the opening of the Ellice basin to the west (Figure 1). The configuration in Figure 11b is that corresponding to 1200 km of separation between the Hikurangi and Manihiki plateaus. The east-west component of spreading explains the east-west offset of the plateaus described by *Eagles et al.* [2004]. This spreading direction also closely parallels the 14° trend of the Southeast Manihiki Scarp. The Southeast Manihiki scarp also appears to be the location of the boundary between the Northern PAC-PHO and Manihiki abyssal hills. In agreement with the results presented by *Larson et al.* [2002], our measurements of the trend of PAC-PHO abyssal hills indicate that the spreading southeast of the Manihiki Plateau occurred along an azimuth of 168° and later rotated to 164° as the PAC-PHO ridge migrated southward. The different spreading directions observed southeast and southwest of the Manihiki Plateau imply that these regions were created at different plate boundaries, and therefore there were at least three plates separated by these boundaries. These three plates consisted of the plate containing the Manihiki Plateau

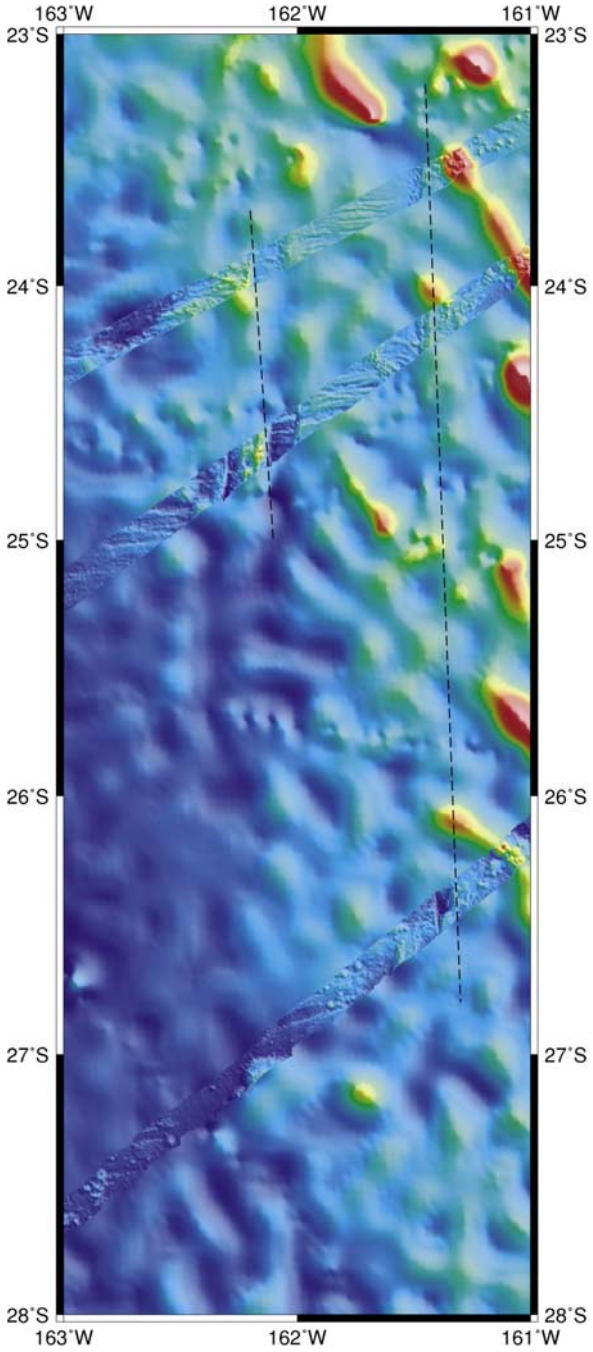

Figure 9. Bathymetric detail of a region east of the Osbourn Trough showing the presence of two bathymetric lineations (marked by dashed lines) that may mark the location of fracture zones. These features may be continuous with either the Southeast Manihiki Scarp or the Pacific-Phoenix-Charcot triple junction trace (Figure 1). These features may also mark the most easterly extent of the Hikurangi plate during Chron C34.

which, following Larson et al., we call the Pacific Plate (although which plate should be considered the ancestor of the modern Pacific plate at this time is debatable; the plates containing the Hikurangi, Manihiki, and Ontong Java Plateaus during the Early Cretaceous make up portions of the modern Pacific Plate), the Hikurangi plate, south of the Osbourn paleospreading center, and the Phoenix plate, south of the Cretaceous Pacific-Phoenix ridge. The boundary between the Hikurangi plates and the Phoenix plates appears to have been at the location of the Southeast Manihiki Scarp, although the exact configuration of this triple junction between the three plates cannot be determined from our data. In Figure 10b we also show the location of the Western Wishbone Scarp as conjugate to the Southeast Manihiki Scarp and therefore it may also be a remnant of the Hikurangi-Phoenix plate boundary. This configuration is in agreement with the fracture zone origin of the West Manihiki Scarp presented by *Mortimer et al.* [2006]. Determining the exact role of the two ridges, and the nature of the boundaries between them, requires more detailed marine geophysical surveys of the West Wishbone Scarp, Southeast Manihiki Scarp and surrounding areas.

[51] After a total of ~2400 km of spreading between the Plateaus, the spreading direction changed to 2°–5° relative to the Manihiki Plateau. Following this rotation another ~900 km of crust was accreted at the Osbourn ridge before the spreading rate of the ridge slowed. The configuration of

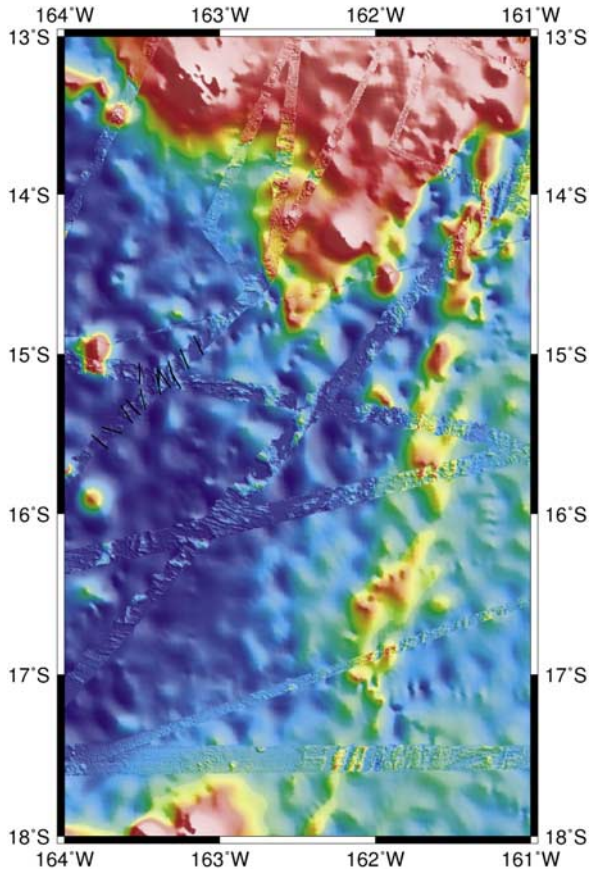

Figure 10. Bathymetry of the southern Manihiki Plateau and Southeast Manihiki Scarp. The short black lines mark the locations of several anomalous ridges that parallel neither the local abyssal-hill fabric nor the trend of the scarp. These features are isolated to this region and because they are subparallel to the southwest side of the Manihiki Plateau, they may have resulted from the rifting that initially separated the Hikurangi and Manihiki Plateaus.

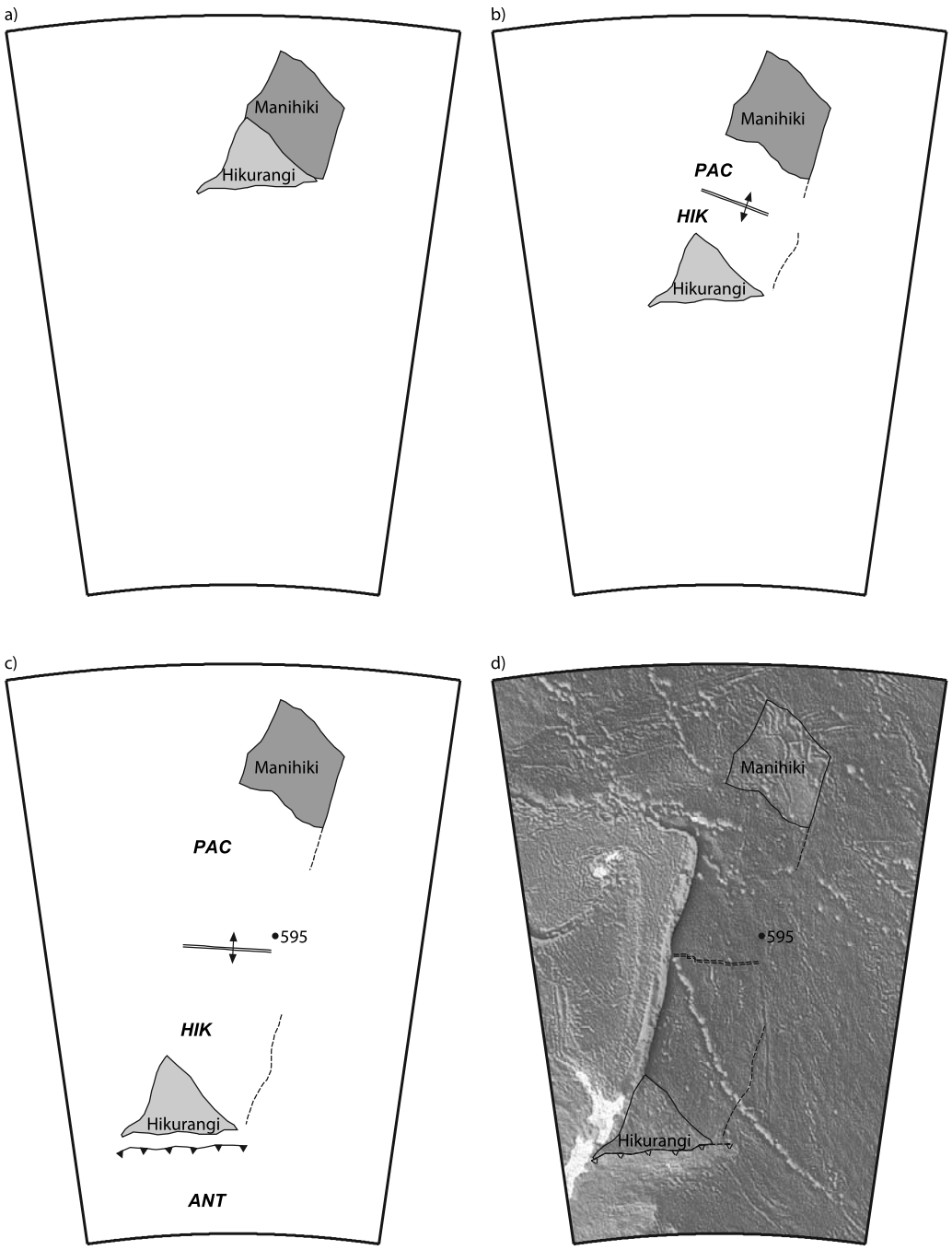

Figure 11. Tectonic model of the Osbourn region, presented in a Manihiki Plateau reference frame. Our model begins with the Hikurangi and Manihiki Plateaus conjugate, in agreement with *Taylor*'s [2006] model. Spreading directions determined by abyssal-hill strikes are shown as double-headed arrows and the locations of the Southeast Manihiki and Western Wishbone Scarps are outlined with dashed lines. The Pacific Plate is labeled PAC, the Hikurangi plate is HIK, and the Antarctic sector of Gondwana is ANT. (a) Beginning location for the Manihiki and Hikurangi plateau. (b) Configuration after 1200 km of total separation between the Plateaus. The spreading direction during the early history of the Osbourn spreading center roughly parallels the strike of the West Wishbone Scarp and the Southeast Manihiki Scarp. The formation of these scarps may be related to the plate boundary that existed here at this time, as implied by the differing azimuths of abyssal hills east and west of the Southeast Manihiki Scarp. (c) The configuration of the Osbourn Spreading center immediately prior to the slowing of spreading. By this time the crust at DSDP site 595 has formed. (d) The configuration of the Osbourn region at the time of extinction of the Osbourn Trough superimposed on the bathymetry of the Southwest Pacific Basin.

the Osbourn region immediately prior to this slowing event is shown in Figure 11c. At no location are the abyssal hills created at the Osbourn spreading center parallel to those created at the Pacific-Phoenix Ridge. Thus it appears that the Hikurangi plate remained separated from the Phoenix Plate throughout its entire lifetime. The fracture zones observed in Figure 9 may mark the location of the eastern-most extent of the Hikurangi Plate at the time of Figure 11c.

[52] We propose, following *Lonsdale* [1997], that the slowing event and eventual extinction of the Osbourn Trough was caused by the entrance of the Hikurangi Plateau into a subduction zone that underthrust the Gondwana section of the Antarctic Plate.

[53] Figure 11d shows the configuration of the spreading center and subduction zone at the time of extinction of the Osbourn Trough, overlain on their modern locations on the Pacific Plate. After the capture of the Hikurangi Plate by the Pacific Plate, the relative motion between the Pacific Plate and Gondwana was divergent; the captured piece began to move northward away from Gondwana. This motion was accommodated by extension in the Zealandia sector of Gondwana as outlined by *Luyendyk* [1995]. Extension continued until ~85 Ma when the Campbell Plateau and Chatham Rise rifted away from Antarctica at the modern Pacific-Antarctic Ridge.

[54] It may have been possible that as the Osbourn spreading center died, the eastern arm of the Wishbone Scarp began forming. As the Hikurangi Plateau entered the subduction zone, it stalled subduction at this location causing the drastic reduction in spreading rate at the western part of the Osbourn ridge. A piece of the eastern part of the Hikurangi Plate may have continued to move southward into the subduction zone, eventually becoming the Charcot Plate of *Eagles et al.* [2004]. In such a scenario the eastern arm of the Wishbone Scarp would have been the location of a strike-slip boundary between the Charcot Plate and the (now captured) Hikurangi portion of the Pacific Plate. However, as there are few data in the region surrounding the Wishbone scarp, such a model remains speculative and is omitted from Figure 11.

6.2. Timing of Osbourn Spreading

[55] Despite their strong geometrical constraints on Osbourn spreading, our data provide little temporal constraint on the events of Figure 11. The magnetic anomaly profiles of Figure 3 imply that the extinction of the Osbourn Spreading Center occurred some time during Chron C34. Abyssal-hill statistics show that spreading at the Osbourn spreading center slowed significantly 2–6 Ma prior to extinction. This slowing event is expressed as a change in the average abyssal-hill amplitude near 25°S north of the Osbourn Trough (Figure 2b). Sediment thickness in the region of Figure 2 is constant at about 60–70 m, so the increased smoothness north of 25°S cannot result from increased sedimentation. We estimate a spreading rate of 2–6 cm/yr FSR after the slowing event and >7 cm/yr FSR prior to slowing, based upon abyssal-hill amplitudes; however, the exact rate before slowing cannot be determined.

[56] We must therefore rely on other data to constrain the timing of these events. One such constraint is provided by the age of the crust at DSDP site 595. Preliminary work estimated a 100 Ma minimum age of the crust at this site [*Menard et al.*, 1987]. *Sutherland and Hollis* [2001], however, estimate the crust at this site to be 132–144 Ma based upon biostratigraphy of cored sediments. Previous models of the Osbourn spreading center have assumed that rifting between the Hikurangi and Manihiki plateaus began shortly after their formation around 119–121 Ma. However, *Mortimer et al.* [2006] show that this rifting only needs to have occurred before the formation of the West Wishbone Scarp at ca. 115 Ma.

[57] A minimum spreading rate of 7 cm/yr FSR for the early portion of Osbourn spreading implies that the crust between the Manihiki Plateau and 25°S, and its conjugate south of 27°S and north of the Hikurangi Plateau, was created in at most 22 Ma. This period, along with the 2–6 Ma period of slow spreading, implies that the Osbourn paleo-spreading center was active for, at most, 24–28 Ma. If rifting began at 121 Ma, extinction of the Osbourn Trough must have occurred by 93–97 Ma. However, if rifting occurred later, at 115Ma, extinction could have been as late as 87–91 Ma. All of these ages are well before the end of Chron C34 at 83 Ma. If the crust at DSDP site 595 was created at the Osbourn spreading center then rifting ages of 121 Ma and 115 Ma predict that the age of this crust is older than 101 Ma and 95 Ma, respectively. Both of these age constraints are in agreement with the age estimates for DSDP site 595 of both *Menard et al.* [1987] and *Sutherland and Hollis* [2001]. The age estimate of *Sutherland and Hollis* [2001] implies that the crust at DSDP site 595 formed prior to the eruption of the Hikurangi and Manihiki Plateaus, an assertion that is difficult to explain if this crust was indeed formed at the Osbourn Trough. However, our data do not directly contradict the model of *Sutherland and Hollis* [2001]. The one ship track that we do have at the longitude of DSDP site 595 shows no evidence of the fracture zone implied by *Sutherland and Hollis* [2001]; however, data in this region are too sparse to eliminate its presence entirely. In the context of their model, the scenario presented in Figure 11 describes the late evolution of the Pacific-Moa plate boundary. Another explanation for the anomalous ages determined by *Sutherland and Hollis* [2001] is that deep sea currents transported older sediments to the location of DSDP site 595.

7. Conclusions

[58] Our data analysis yields several important clues to explaining the tectonic history of the Osbourn Trough. Analysis of the magnetic data shows that the Osbourn paleospreading center stopped spreading during Chron C34. The most fruitful part of our analysis is the examination of the seafloor fabric away from the trough axis. A change in seafloor RMS amplitude shows that spreading slowed 2–6 Ma prior to the extinction of the Osbourn Trough. Change in abyssal-hill strike also shows that spreading direction changed from NNE-SSW to approximately N-S (measured in a modern Manihiki Plateau reference frame) some time prior to the slowing event. Using our results, we formulated a new model of the Osbourn Trough's tectonic history.

[59] Our model successfully explains the conflict between Osbourn paleospreading models and regional models by

showing that spreading on the Osbourn spreading center was decoupled from that of the Pacific-Phoenix Ridge and by showing that the Osbourn spreading center spread at a rate faster than predicted by its axial characteristics. Correspondingly, our model predicts that the Osbourn spreading center ceased spreading prior to previous estimates. A rifting age of 115 Ma for the Hikurangi and Manihiki Plateaus predicts spreading ceased prior to 87 Ma, while a 121 Ma extinction age implies that spreading stopped before 93 Ma.

[60] One aspect of our tectonic model warranting further study is the interaction of the western end of the Pacific-Phoenix Ridge with the Ellice Basin spreading center postulated to be active at this time [*Taylor*, 2006]. The presence of the Ellice Ridge implies that there must be a triple junction trace somewhere southwest of the Manihiki Plateau, although no such feature has been identified. As this region is heavily sedimented and has been subject to much intraplate volcanism further marine geophysical surveys are required to elucidate the details of formation of this area. The Wishbone Scarp is also sparsely surveyed, and more data are required to determine the origin of this anomalous feature. Another aspect warranting further investigation is the extent of the fracture zones of Figure 9 and whether they are contiguous with either the Southeast Manihiki Scarp or the Charcot-Phoenix-Pacific triple junction trace described by *Eagles et al.* [2004].

Appendix A: Effect of Sedimentation on Spreading Rates and Direction Estimates From Abyssal-Hill Fabric

[61] Our seismic data provide a means to quantify the effects of sedimentation on abyssal-hill statistics. The NBP0207 seismic line runs north-south perpendicular to the trend of the abyssal-hill fabric. The two-dimensional nature of the seafloor morphology perpendicular to the seismic line implies that the observed seismic bathymetry and basement depth are a good approximation to the average bathymetry and basement topography along an azimuth of 90° (i.e., the bathymetry and basement topography along the seismic line is expected to be similar in shape to the Radon transform of the two-dimensional bathymetry and basement topography at $\theta = 90°$). The unusual fabric near the NBP0304b seismic lines precludes their use in this analysis because the bathymetry along the seismic line is not representative of the bathymetry across the NBP0304b multibeam swath.

[62] By comparing the RMS amplitude and scales of the seismically determined bathymetry and basement topography profiles, we are able to determine the effect of sedimentation on these quantities. Figure S1a[1] shows the bathymetry and basement topography interpreted from the NBP0207 seismic data. Figure S1b shows the sediment thickness observed along this line after the application of a mean filter of 5 km half-width. Figure S1c displays the ratio of the bathymetry RMS amplitude to the basement RMS amplitude, each of which have been calculated using a 20 km moving window. The rough negative correlation between this ratio and the sediment depth in Figure S1b indicates that thicker sediments reduce the RMS amplitude of the bathymetry relative to that of the basement more effectively than do thinner sediments. Furthermore, where sediment thickness is less than 75–100 m, the ratio in Figure S1c is very near to 1, indicating that a sediment cover of this thickness does not significantly reduce the RMS amplitude of the bathymetry relative to the RMS amplitude of the basement. Similar results have been reported by *Goff* [1991], *Goff and Tucholke* [1997], and *Goff et al.* [1995] and are predicted by the sedimentation model of *Webb and Jordan* [1993].

[63] Figures S1d–S1f demonstrate the effects of sedimentation on scale. Figures S1d and S1e are the wavelet transforms of the basement topography and bathymetry respectively. Figure S1f is the difference between Figure S1d and S1e. The two wavelet transforms are very similar in shape, but their amplitudes differ for widths less than 8 km (Figure S1f). Thus the effect of sedimentation is to preferentially reduce the features of small scale. We do not observe a correlation between the range of scales affected and the sediment thickness. Such a correlation has been observed by *Goff* [1991] and *Goff et al.* [1997, 1995], where sediments progressively dampen larger scales with increasing sediment thickness.

[64] In order to accurately interpret the results of our multibeam analysis it is important to know the sediment thickness near our survey locations. Where sediments are relatively thin (<70–100 m) we can be confident that our RMS amplitude is an accurate estimate of the RMS amplitude of basement. Our scale measurements will be affected by sedimentation regardless of sediment depth. Where possible we can use our seismically determined sediment thickness. Elsewhere we must rely on the NGDC global sediment thickness database [*Divins*, 2006]. Sedimentation, however, should have no effect on abyssal-hill azimuths because sedimentation acts to change abyssal-hill widths and amplitudes only.

[65] **Acknowledgments.** The Palmer cruises were supported by NSF grant OPP-0126334. Subsequent data analysis was supported by NSF grant OPP-0338317. We thank the Captain and crew of both the *R/VIB Nathaniel B. Palmer* and the *R/V Kilo Moana*. Brian Taylor provided us the opportunity to participate in, and use data from, cruise KM0413. We also thank Steve Miller for permission to use the COOK20 data. We thank Brian Taylor and an anonymous reviewer for insightful reviews that greatly improved this paper. California Institute of Technology Division of Geological and Planetary Sciences, contribution number 9148.

References

Billen, M., and J. Stock (2000), Morphology and origin of the Osbourn Trough, *J. Geophys. Res.*, *105*, 13,481–13,489.

Bowers, N., et al. (2001), Fluctuations of the paleomagnetic field during Chron C5 as recorded in near-bottom marine magnetic anomaly data, *J. Geophys. Res.*, *106*, 26,379–26,396.

Buck, W., and A. Polikov (1998), Abyssal hills formed by stretching oceanic lithosphere, *Nature*, *392*, 272–275.

Burns, R., et al. (1973), *Initial Reports of the Deep-Sea Drilling Program*, vol. 21, U.S. Gov. Print. Off., Washington, D. C.

Cande, S., and D. Kent (1995), Revised calibration of the geomagnetic polarity time scale for the late Cretaceous and Cenozoic, *J. Geophys. Res.*, *100*, 6093–6095.

Candès, E. (1998), Ridgelets: Theory and application, Ph.D. thesis, 116 pp., Stanford Univ., Stanford, Calif.

Candès, E., and D. Donoho (1999), Ridgelets: A key to higher dimensional intermittency, *Philos. Trans. R. Soc. London*, *357*, 2495–2509.

Divins, D. L. (2006), Total Sediment Thickness of the World's Oceans & Marginal Seas, http://www.ngdc.noaa.gov/mgg/sedthick/sedthick.html, World Data Cent. for Mar. Geol. and Geophys., Boulder, Colo.

[1] Auxiliary materials are available in the HTML. doi:10.1029/2006JB004550.

Downey, N. J., and R. W. Clayton (2007), A ridgelet transform method for constraining tectonic models via abyssal-hill morphology, *Geochem. Geophys. Geosyst.*, *8*, Q03004, doi:10.1029/2006GC001440.

Eagles, G., K. Gohl, and R. D. Larter (2004), High-resolution animated tectonic reconstruction of the South Pacific and West Antarctic Margin, *Geochem. Geophys. Geosyst.*, *5*, Q07002, doi:10.1029/2003GC000657.

Elthon, D., et al. (1982), Mineral chemistry of ultramafic cumulates from the North Arm Mountain massif of the Bay of Islands ophiolite: Evidence for high-pressure crystal fractionation of oceanic basalts, *J. Geophys. Res.*, *87*, 8717–8734.

Goff, J. (1991), A global and regional stochastic analysis of near-ridge abyssal hill morphology, *J. Geophys. Res.*, *96*, 21,713–21,737.

Goff, J., and T. H. Jordan (1988), Stochastic modeling of seafloor morphology: Inversion of Sea Beam data for second-order statistics, *J. Geophys. Res.*, *93*, 13,589–13,608.

Goff, J., and B. Tucholke (1997), Multiscale spectral analysis of bathymetry on the flank of the Mid-Atlantic Ridge: Modification of the seafloor by mass wasting and sedimentation, *J. Geophys. Res.*, *102*, 15,447–15,462.

Goff, J., et al. (1995), Quantitative analysis of abyssal hills in the Atlantic Ocean: A correlation between inferred crustal thickness and extensional faulting, *J. Geophys. Res.*, *100*, 22,509–22,522.

Goff, J., et al. (1997), Stochastic analysis of seafloor morphology on the flank of the southeast Indian Ridge: The influence of ridge morphology on the formation of abyssal hills, *J. Geophys. Res.*, *102*, 15,521–15,534.

Hayes, D., and K. Kane (1991), The dependence of seafloor roughness on spreading rate, *Geophys. Res. Lett.*, *18*, 1425–1428.

Hoernle, K., et al. (2004), New insights into the origin and evolution of the Hikurangi oceanic plateau, *Eos Trans. AGU*, *85*, 401.

Jonas, J., et al. (1991), Gravity anomalies over spreading centers: A test of gravity models of active centers, *J. Geophys. Res.*, *96*, 11,759–11,777.

Jung, W., and P. Vogt (1997), A gravity and magnetic anomaly study of the extinct Aegir Ridge, Norwegian Sea, *J. Geophys. Res.*, *102*, 5065–5089.

Kriner, K., et al. (2006), Bathymetric gradients of lineated abyssal hills: Inferring seafloor spreading vectors and a new model for hills formed at ultra-fast rates, *Earth Planet. Sci. Lett.*, *242*, 98–110.

Larson, R., et al. (2002), Mid-Cretaceous tectonic evolution of the Tongareva triple junction in the southwest Pacific Basin, *Geology*, *30*, 67–70.

Larter, R. D., A. P. Cunningham, P. F. Barker, K. Gohl, and F. O. Nitsche (2002), Tectonic evolution of the Pacific margin of Antarctica: 1. Late Cretaceous tectonic reconstructions, *J. Geophys. Res.*, *107*(B12), 2345, doi:10.1029/2000JB000052.

Lonsdale, P. (1997), An incomplete geologic history of the south-west Pacific Basin, *Geol. Soc. Am. Abstr. Programs*, *29*, 4574.

Luyendyk, B. (1995), Hypothesis for Cretaceous rifting of east Gondwana caused by subducted slab capture, *Geology*, *23*, 373–376.

Macdonald, K., et al. (1991), Mid-ocean ridges: Discontinuities, segments and giant cracks, *Science*, *253*, 986–994.

Macdonald, K., et al. (1996), Volcanic growth faults and the origin of Pacific abyssal hills, *Nature*, *380*, 125–129.

Menard, H. W. (1967), Sea floor spreading, topography and the second layer, *Science*, *157*, 923–924.

Menard, H. W., et al. (1987), *Initial Reports of the Deep-Sea Drilling Program*, vol. 91, U.S. Gov. Print. Off., Washington, D. C.

Mortimer, N., and D. Parkinson (1996), Hikurangi plateau: A Cretaceous large igneous province in the southwest Pacific Ocean, *J. Geophys. Res.*, *101*, 687–696.

Mortimer, N., et al. (2006), New constraints on the age and evolution of the Wishbone Ridge, southwest Pacific Cretaceous microplates, and Zealandia-West Antarctica breakup, *Geology*, *34*, 185–188.

Müller, R. D., S. C. Cande, J. M. Stock, and W. R. Keller (2005), Crustal structure and rift flank uplift of the Adare Trough, Antarctica, *Geochem. Geophys. Geosyst.*, *6*, Q11010, doi:10.1029/2005GC001027.

Nettleton, L. (1939), Determination of density for reduction of gravimeter observations, *Geophysics*, *4*, 176–183.

Osler, J., and K. Louden (1992), Crustal structure of an extinct rift axis in the Labrador Sea: Preliminary results from a seismic refraction survey, *Earth Planet. Sci. Lett.*, *108*, 243–258.

Parker, R. (1972), The rapid calculation of potential anomalies, *Geophys. J. R. Astron. Soc.*, *31*, 447–455.

Sandwell, D. T., and W. H. F. Smith (1997), Marine gravity anomaly from Geosat and ERS-1 satellite altimetry, *J. Geophys. Res.*, *102*, 10,039–10,054.

Small, C. (1994), A global analysis of mid-ocean ridge axial topography, *Geophys. J. Int.*, *116*, 64–84.

Small, C., and D. Abbott (1998), Subduction obstruction and the crack-up of the Pacific plate, *Geology*, *26*, 795–798.

Smith, W. H. F., and D. T. Sandwell (1997), Global sea floor topography from satellite altimetry and ship depth soundings, *Science*, *277*, 1956–1962.

Srivastava, S., and C. Keen (1995), A deep seismic reflection profile across the extinct Mid-Labrador Sea spreading center, *Tectonics*, *14*, 372–389.

Sutherland, R., and C. Hollis (2001), Cretaceous demise of the Moa plate and strike-slip motion at the Gondwana margin, *Geology*, *29*, 279–282.

Taylor, B. (2006), The single largest oceanic plateau: Ontong Java-Manihiki-Hikurangi, *Earth Planet. Sci. Lett.*, *241*, 372–380.

Uenzelmann-Neben, G., et al. (1992), The Aegir Ridge: Structure of an extinct spreading axis, *J. Geophys. Res.*, *97*, 9203–9218.

Watts, A. (1982), Gravity anomalies over oceanic rifts, in *Continental and Oceanic Rifts*, *Geodyn. Ser.*, vol. 8, edited by G. Palmeson, pp. 99–105, AGU, Washington, D. C.

Watts, A. (2001), *Isostasy and Flexure of the Lithosphere*, 458 pp., Cambridge Univ. Press, New York.

Webb, H., and T. H. Jordan (1993), Quantifying the distribution and transport of pelagic sediments on young abyssal hills, *Geophys. Res. Lett.*, *20*, 2203–2206.

Zar, J. (1999), *Biostatistical Analysis*, Prentice-Hall, Upper Saddle River, N. J.

S. C. Cande, Scripps Institution of Oceanography, 9500 Gilman Drive, La Jolla, CA 92093, USA.

R. W. Clayton, N. J. Downey, and J. M. Stock, Seismological Laboratory, California Institute of Technology, 1200 E. California Boulevard, 252-21, Pasadena, CA 91125, USA. (ndowney@gps.caltech.edu)